Proceedings of Basic and Applied Sciences
ISSN 1857-8179 (paper). ISSN 1857-8187 (online). http://www.anglisticum.mk
Proceedings of the 1st International Conference on New Horizons in Basic and Applied Science, Hurghada – Egypt, Vol 1(1), 2013.

Structural and Optical Properties of Varies Thickness of Znte Nanoparticle

E. R. Shaaban[1], M. Ahmad[1], E. A. Abdel Wahab[1], H.Shokry Hassan[2], A.M.Aboraia[1]
1 Physics Department, Faculty of Science, Al-Azhar University, Assuit, 71542, Egypt
2 Advanced Technology and New Materials Research Institute, City of Scientific Research and Technology Applications, New Borg El-Arab City, Alexandria 21934, Egypt. *E-mail of the Corresponding author: esam_ramadan2008@yahoo.com

Received November 13, 2013; Revised November 14, 2013; Accepted November 15, 2013

Abstract: *ZnTe thin films of different thicknesses were deposited onto glass substrates for optical devices applications. X-ray diffractogram of different thicknesses for ZnTe films are measured and their patterns exhibits polycrystalline nature with a preferential orientation along the (111) plane. X-ray diffraction techniques have been employed to determine the microstructure parameters, both crystallite size and microstrain. Film thickness and the optical constants of ZnTe films were calculated based on the measured transmittance spectral data using Swanepole's method in the wavelength range 400–2500 nm. The refractive index n and absorption index k were calculated and the refractive index exhibits a normal dispersion. The refractive index could be extrapolated by Cauchy dispersion relationship over the whole spectra range, which extended from 400 to 2500 nm. The optical band gap can be calculated in strong absorption region and displays an allowed direct transition. Both the refractive index and the band gap increase with the increase film thickness, thus ZnTe/glass substrates are good candidates in optoelectronic devices.*

Keywords: *ZnTe, thin film, cry crystallitze size; microstrain; optical constants.*

Introduction

ZnTe has the direct bandgap of 2.26 eV and zinc-blend structure with a lattice constant of 6.104 Ǻ, and is one of the promising II–VI materials for optoelectronic devices, such as pure green lightemitting diodes, solar cells, and terahertz detectors [W.L.Wolfe (1978), J. De Merchant et al (1996) A. Kaneta et al (2000)]. The deposition time, namely thickness, greatly influence the crystal structure, composition and morphology of the films which in turn affect the electric and opto-electric properties of films.Film thickness is an important parameter in determining the efficiency of optical devices, e.g. interference filter, buffer layers for IR detectors, as back contact for thin films solar cell and opto-electronic devices all of which depend on the variation in optical properties with film thickness. Moreover, the optical properties are closely related to the structure of the films and study of the optical properties gives valuable information about the latter properties. Thin films of ZnTe have been prepared by different techniques, such as thermal evaporation [A. Pistone et al (1998)], hot wall evaporation [A. Mondal(1978)], rf sputtering [H. Bellakhder et al,(2001)], molecular beam epitaxy [R.L. Gunshor et al(1986)] and electrodeposition [T. Ishizaki, et al (2004)]. The thermal evaporation is considered to be a standard and reproducible method for the preparation of thin films of ZnTe [A. Pistone et al (1998), C.T. Lynch (Ed.) et al (1974), Coating Materials (1981), A.A. Ibrahim(2004).]. the present work has twofold purpose: the first purpose is to study the effect of film thickness on both microstructure parameter (crystallite size and microstrain) and optical constants of ZnTe thin films obtained by vacuum evaporation. The second purpose is to interpret the behavior of the optical constants on microstructure parameters of the films.

© The authors. Published by Info Media Group & Anglisticum Journal, Tetovo, Macedonia.
Selection and peer-review under responsibility of ICNHBAS, 2013 http://www.nhbas2013.com

Experimental

Different thickness thin films were deposited by evaporating pure ZnTe compound (99.995%, purchased from Aldrich) from a resistance heating quartz glass crucible onto ultrasonically cleaned glass substrates kept at constant room temperature, using a conventional coating unit (Denton Vacuum DV 502 A) and a vacuum of about 10^{-6} Pa. The mechanical rotation of the substrate holder (≈30 rpm) produced homogeneous films. The evaporation rate as well as the film thickness was controlled using a quartz crystal DTM 100 monitor. The deposition rate was maintained 5 Å/s constant throughout the sample preparations. Such a low deposition rate produces a film composition, which is very close to that of the bulk starting material. The film thickness was precalibrated with multiplebeam Fizeau fringes at reflections. The structure of the prepared samples were examined by XRD analysis (Philips X-ray diffractometry 1710) with Ni-filtered Cu Kα radiation with λ = 0.15418 nm). The intensity data were collected using the step scanning mode with a small interval (Δ2θ=0.02o) with a period of 10 s at each fixed value to yield reasonable number of counts at each peak maximum. The full width at half-maximum (FWHM) was determined to a high degree of precision by a program Origin version 7 (OriginLab Corp.). The transmittance $T(\lambda)$ and reflectance $R(\lambda)$ measurements were carried out using a double-beam (Shimadzu UV-2101 combined with PC) computer-controlled spectrophotometer, at normal incidence of light and in a wavelength range between 400 and 2500 nm. The spectrophotometer was (Shimadzu UV-2101) provided with a V-N absolute specular reflection attachment. Without a glass substrate in the reference beam, the measured transmittance spectra were used to calculate the refractive index and the film thickness of ZnTe thin films.

Results and discussion

Determination of microstructure

Parameters: The XRD patterns of ZnTe films of various thicknesses deposited on glass substrates aer shown in Fig. 1The X-ray diffraction (XRD) analysis revealed that the films are polycrystalline of zinc-blende structure with peaks at 2θ = 25.42°, 42.20°, 49.87° and 67.14° corresponding to C(1 1 1), C(2 2 0), C(3 1 1) and C(331) orientations, respectively (JCPDS Data file: 01-0582-cubic). It can be seen that the film thickness affects the XRD pattern of ZnTe thin films i.e. the peak intensity increases with increasing film thickness. Each X-ray diffraction line profile is broadened due to instrumental and physical factors (crystallite size and lattice strains) [H. P. Kluge et al(1974)]. Therefore, the first indispensable preparatory step to the calculation of crystallite size and lattice strain from the recorded XRD scan is the determination of the "pure" diffraction line profile for a given reflection whose full-width at half maximum (FWHM) depends solely on the physical factors [H. P. Kluge et al(1974)]. This "pure" line profile is extracted by removing (deconvoluting) the instrumental broadening factor from the experimental line profile. Only then the "pure" line profile can be used for calculating the crystallite size and lattice strain. Simple equations or graphs based on line profiles of assumed analytical forms can be used for the instrumental broadening correction [H. P. Kluge et al(1974)].

© The authors. Published by Info Media Group & Anglisticum Journal, Tetovo, Macedonia.
Selection and peer-review under responsibility of ICNHBAS, 2013 http://www.nhbas2013.com

In the present work, the instrumental broadening-corrected "pure" FWHM of each reflection was calculated from the parabolic approximation correction [H. P. Kluge et al(1974)]:

$$\Delta 2\theta = B\left(1 - \frac{b^2}{B^2}\right)(rad) \qquad (1)$$

where *B* and *b* are the FWHM (in radians) of the same Bragg-peak from the XRD scans of the experimental and reference powder, respectively. The XRD pattern of the reference powder (the starting ZnTe powdered and annealed at 300°C for 2 h) and simulated references code by Retiveld refinement are shown in Fig. 2. Table 1 illustrates the values of $\Delta(2\theta_0)$ for each reflection at different ZnTe film thicknesses. The full-width at half maximum (FWHM) was found to decrease at each reflection with increasing film thickness as shown in Fig. 2. Such behavior reflects the decreased contribution of latticeimperfections. This may due to a decrease in internal microstrain within the film and an increase in the crystallite size. In the following this will be confirmed quantitatively.
The method was based on the assumption that the crystallite size and strain line profiles are both presumed to be Cauchy and the appropriate equation for the separation of crystallite size and strain

takes the following form [H. P. Kluge et al(1974)]: $\Delta(2\theta_0)cos\theta = \frac{k\lambda}{D_v} + 4e(sin\theta_0) \quad (2)$

Fig. 3 illustrates the plot of $\Delta(2\theta_0)\ cos\theta_0$ vs $sin\theta_0$ and the values of *e* and D_v can be calculated from the slope and the ordinate intersection respectively. Eq. (2) was first proposed by Williamson and Hall [G. K. Williamson(1953)] and is customarily referred to as the "Williamson- Hall method" [D.G. Morris et al (1992), G. H. Chen et al (1995) , F. W. Gayle et al (1995), E. Szewczak et al (1997).]. Fig. 4 shows a comparative look of microstructure parameters of both crystallite size (*Dv*) and microstrain of the ZnTe films of different thicknesses deposited on glass substrates. It is observed that the crystallite size increases with the increase of film thickness. On the other hand the microstrain exhibited an opposite behavior, i.e., it decreases with increasing film thickness. Such a decrease in microstrain may be due to the decrease in lattice defects among the grain boundaries with the grain size increasing.

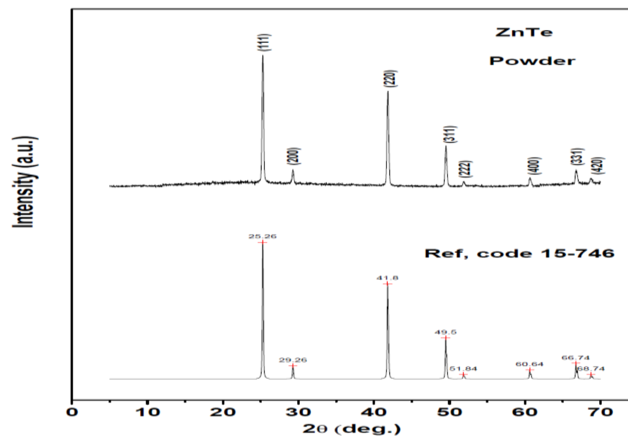

Fig. 1. The XRD patterns of the reference powder of ZnTe.

© The authors. Published by Info Media Group & Anglisticum Journal, Tetovo, Macedonia.
Selection and peer-review under responsibility of ICNHBAS, 2013 http://www.nhbas2013.com

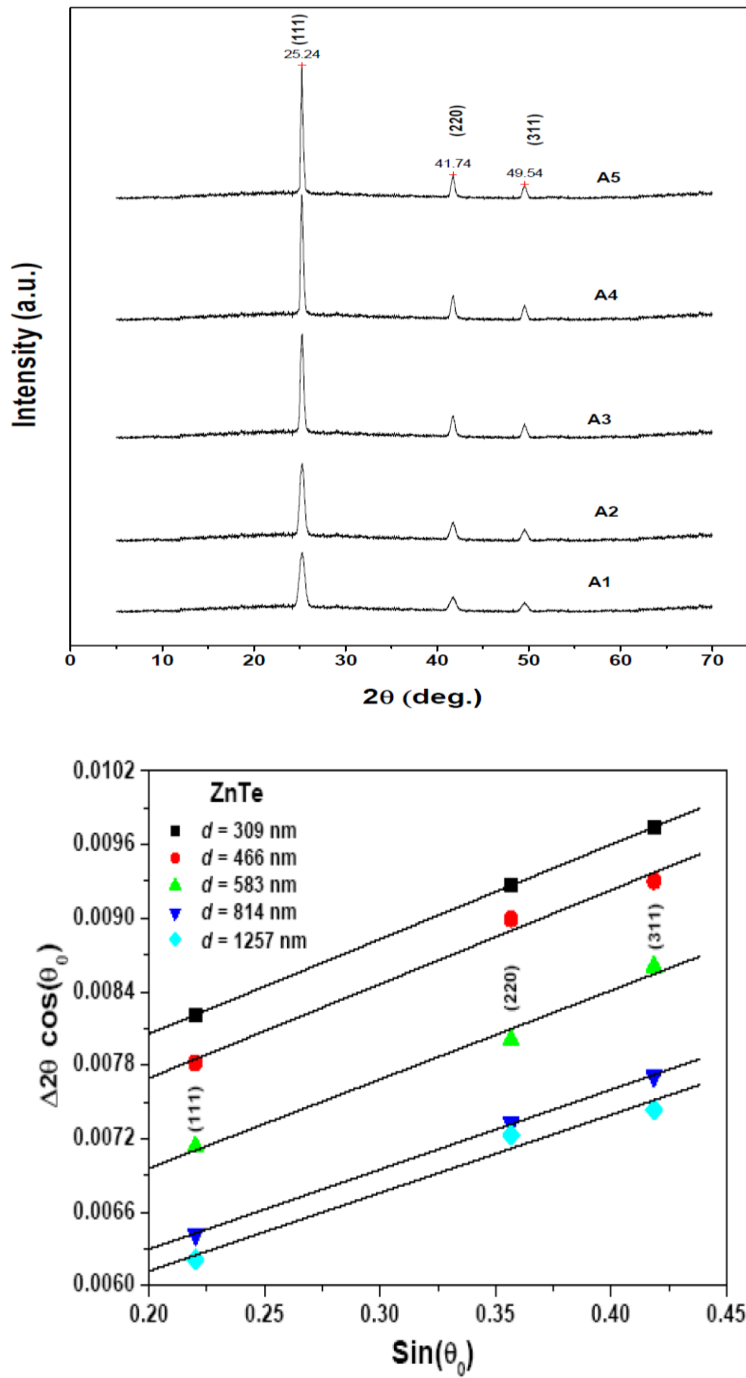

Fig. 3. Crystallite size/strain separation calculating using $\Delta(2\theta_0)$ breadth according to"Williamson–Hall" method.

© The authors. Published by Info Media Group & Anglisticum Journal, Tetovo, Macedonia.
Selection and peer-review under responsibility of ICNHBAS, 2013 http://www.nhbas2013.com

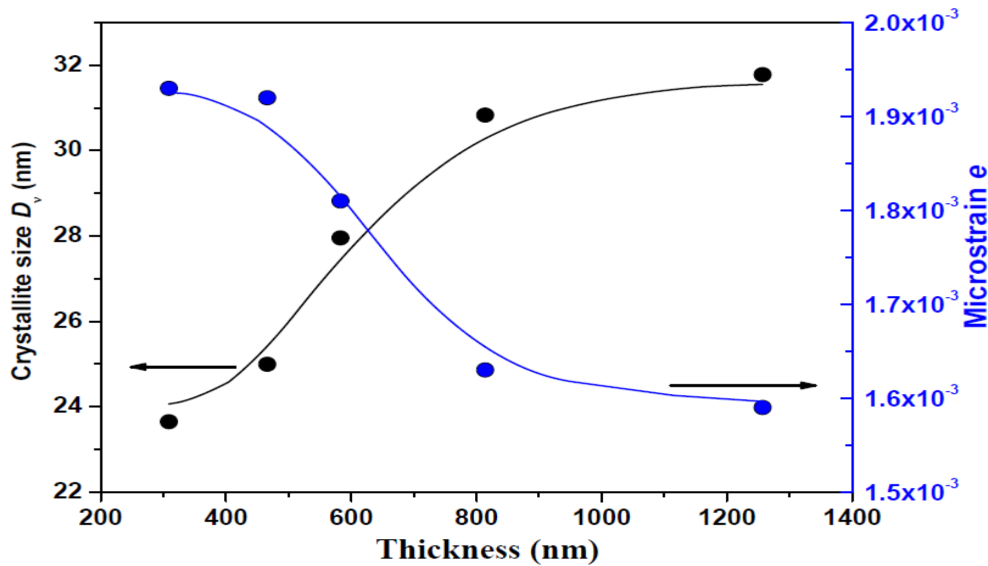

Fig.4. Effect of film thickness on both crystallite size and microstrain of ZnTe thin films.

Optical constants of ZnTe/glass substrate

The transmittance and reflectance spectrum of the deposited films as a function of wavelength are depicted in Fig.5. It can be seen that the non-shrinking interference fringes (fringes of equal chromatic order FECO) observed in transmittance spectra at longer wavelength (1000-2000 nm) indicate the homogeneity and smoothness of the deposited films. Furthermore, the absorption edge (beginning of absorption process within the film materials) of the deposited films show blue shift as the increasing the film thickness. This shift is a direct consequence of the thickness dependence of the optical transmittance spectra and consequently optical band gap of the deposited films. The envelope method suggested by Swanepoel [R. Swanepoel R(1984)], employed extensively by many researchers[, A.K. Kulkarnia et al(1997), E. R. Shaaban et al (2011), E. Márquez et al (2008), E.R. Shaaban, et al (2008), E. R. Shaaban (2008)], was used to calculate the refractive index and thickness of the thin films. Swanepoel's method based on a creation of top and bottom envelopes to the interference maxima and minima observed in transmittance spectra. A first approximate value of the refractive index of the film n_1, in the spectral region of medium and weak absorption, can be calculated by the expression

$$n_1 = \left[N_1 + (N_1^2 - s^2)^{\frac{1}{2}} \right]^{\frac{1}{2}} \qquad (3)$$

Where $N_1 = 2s \frac{T_M - T_m}{T_M T_m} + \frac{s^2 + 1}{2}$

© The authors. Published by Info Media Group & Anglisticum Journal, Tetovo, Macedonia.
Selection and peer-review under responsibility of ICNHBAS, 2013 http://www.nhbas2013.com

Here T_M and Tm, are the transmission maximum and the corresponding minimum at a certain wavelength λ. Alternatively, one of these values is an experimental interference extreme and the other one is derived from the corresponding envelope; both envelopes were computer-generated using the origin version 7 program using more than one procedure. On the other hand, the necessary values of the refractive index of the substrate. are obtained from the transmission spectrum of the substrate, T_s using the well-known equation:

$$S = \frac{1}{T_s} + (\frac{1}{T_s} - 1)^{1/2} \qquad (4)$$

The values of the refractive index *n,* as calculated from eq. (2) are shown in Table 2. The accuracy of this initial estimation of the refractive index is improved after calculating *d*, as will be explained below. Now, it is necessary to take into account the basic equation for interference fringes

$$2nd = m\lambda \qquad (5)$$

where the order numbers *m* is integer for maxima and half integer for minima. Moreover, if n_{el} and n_{e2} are the refractive indices at two adjacent maxima (or minima) at λ_1 and λ_2, it follows that the film thickness is given by the expression

$$d = \frac{\lambda_1\lambda_2}{2(\lambda_1 n_{e2} - \lambda_2 n_{e1})} \qquad (6)$$

The values of *d* of different samples determined by this equation are listed as d_1, in Table 2. The average value of d_1, (ignoring the last two values). This value can now be used, along with n_1, to calculate the "order number" m_0 for the different extremes using eq. (5). The accuracy of *d* can now be significantly increased by taking the corresponding exact integer or half integer values of *m* associated to each extreme (Fig. 6 a & b) and deriving a new thickness, d_2 from eq. (4), again using the values of n_1, the values of *d* found in this way have a smaller dispersion ($\sigma_1 > \sigma_2$). It should be emphasized that the accuracy of the final thickness is better than 1%. (Table 2**).** With the exact value of *m* and the very accurate value of eq. (4) can then be solved for *n* at each *λ* and, thus, the final values of the refractive index n_2 are obtained (Table 2). Fig. 4 illustrates the dependence of refractive index *n* as a function of wavelength for different thickness of ZnTe thin films. Now, the values of *n* can be fitted to a reasonable dispersion function such as the two-term Cauchy function, $n(\lambda) = a + b/\lambda^2$, which can be used for extrapolation the whole wavelength dependence of refractive index, see Fig.7 [R. Swanepoel R(1984) , employed extensively by many researchers, A.K. Kulkarnia et al(1997), E. R. Shaaban et al (2011), E. Márquez et al (2008), E.R. Shaaban, et al (2008), E. R. Shaaban (2008)]. The least squares fit of the four sets of values of *n* corresponding the four different composition samples, yields $n = 2.400 + 4.93x10^5/\lambda^2$ for A1, $n = 2.470 + 5.54\ x10^5/\lambda^2$ for A2, $n = 2.737 + 5.59\ x10^5/\lambda^2$ for A3 and $n = 2.235 + 4.47\ x10^5/\lambda^2$ for A4, respectively. As clearly seen in Fig.4 the change in the *n* values is related to the change in the film thickness, i.e. the refractive index values increase with increasing the film thickness of ZnTe thin film. The increase in refractive index with increasing film thickness may be attributed to the increased density of the film and increasing in crystallites size.

© The authors. Published by Info Media Group & Anglisticum Journal, Tetovo, Macedonia.
Selection and peer-review under responsibility of ICNHBAS, 2013 http://www.nhbas2013.com

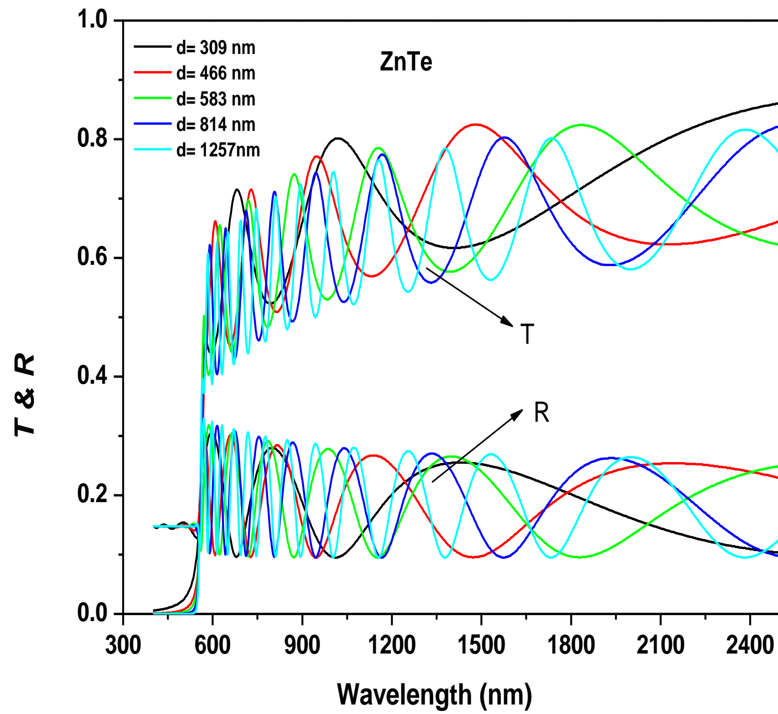

Fig. 5. Transmittance and reflectance spectrum for ZnTe thin films with different thickness.

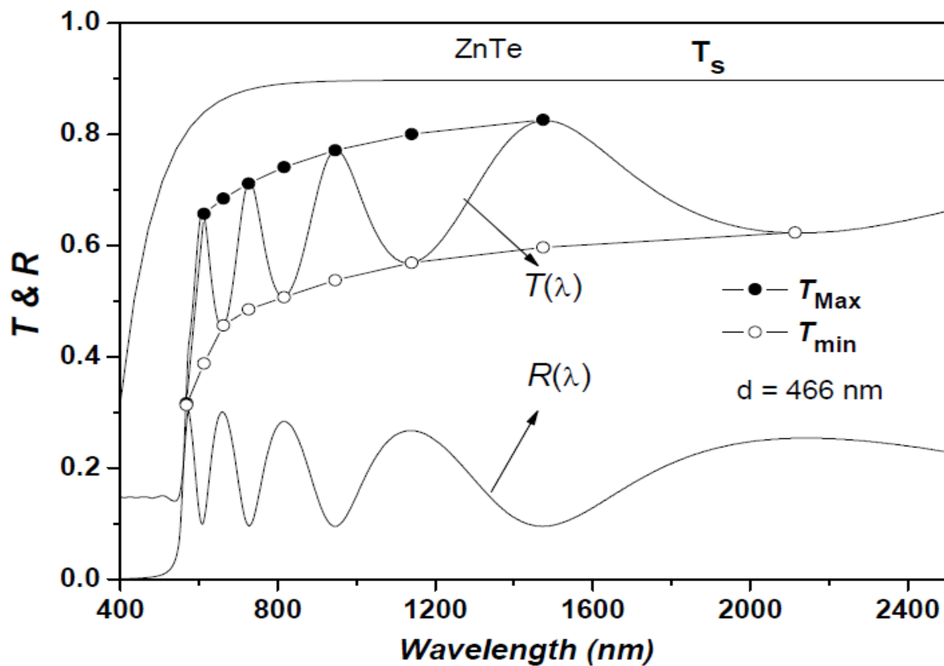

Fig 6a. The typical transmittance spectra of ZnTe thin films for different thicknesses: d = 466 nm. Curve T_M, and T_m, according to the text.

© The authors. Published by Info Media Group & Anglisticum Journal, Tetovo, Macedonia.
Selection and peer-review under responsibility of ICNHBAS, 2013 http://www.nhbas2013.com

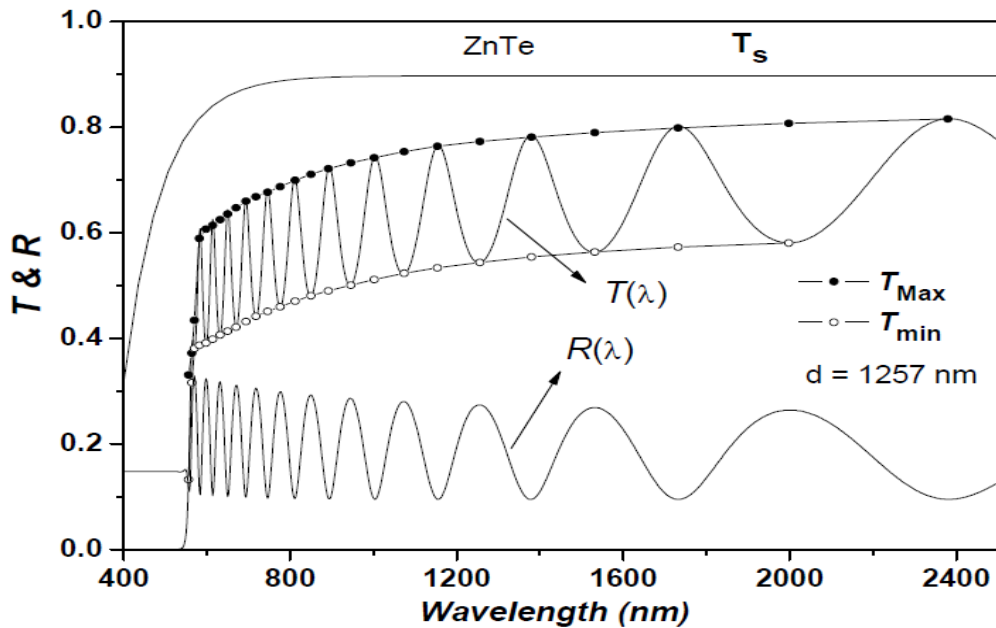

Fig .6b. The typical transmittance spectra of ZnTe thin films for different thicknesses: d = 1257 nm. Curves T_M, and T_m, according to the text.

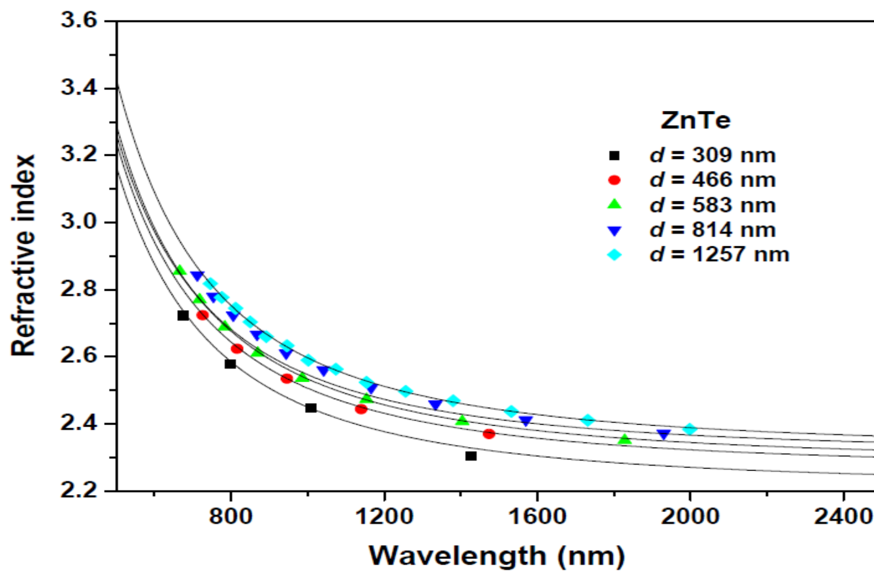

Fig.7. The spectral dependence of refractive index *n* of ZnTe films with different thicknesses (*d*).

© The authors. Published by Info Media Group & Anglisticum Journal, Tetovo, Macedonia.
Selection and peer-review under responsibility of ICNHBAS, 2013 http://www.nhbas2013.com

Determination of the absorption coefficient and the optical band gap of ZnTe

The absorption coefficient, α of different thickness of ZnTe thin film is calculated from the experimental data of transmittance (*T*) and reflectance (*R*) in strong absorption region using the relation [M. Kastner,(1972)]:

$$\alpha = \frac{1}{d}\ln\left[\frac{(1-R)^2 + \left[(1-R)^4 + 4R^2T^2\right]^{1/2}}{2T}\right] \quad (7)$$

where *d* is the sample thickness. Fig.6 shows dependence of the absorption coefficient α(*h*ν) on photon energy as a function of film thickness for ZnTe thin films. It is known that pure semiconducting compounds have a sharp absorption edge (corresponding to forbidden energy bandgap) [) L.L. Kazmersky (Ed.), et al (1980), R. Swanepoel (1983), E. Marques, et al (1995), C. Baban, et al (2003), M. Nowak(1995)] Fig. 8 shows the dependence of the absorption coefficient, α, on photon energy *(h*ν *)* for polycrystalline ZnTe thin films. In Fig. 8, it is clearly observed that the value of the absorption edge increase with increasing the film thickness.The shapes of absorption spectra for ZnTe thin films Show that the respective films have a stoichiometric composition. In order to complete the calculation of the optical constants, the extinction coefficient is estimated from the values of α and λ using the known formula $k = \alpha\lambda/4\pi$. Fig.9 illustrates the dependence of *k* on wavelength for different samples of thin films. It is known, that in the vicinity of the fundamental absorption edge, for allowed direct band-to-band transitions, neglecting exciton effects, the absorption coefficient is described by the

$$\alpha(h\nu) = \frac{k(h\nu - E_g^{opt})^m}{h\nu} \quad (8)$$

where *K* is a characteristic parameter (independent of photon energy) for respective transitions [48], *h*ν denotes photon energy, E_g^{opt} is optical energy gap and *m* is a number which characterizes the transition process. Different authors [E.R. Shaaban, et al (2008), E. R. Shaaban (2008). M. Kastner,(1972), L.L. Kazmersky (Ed.), et al (1980), R. Swanepoel (1983), E. Marques, et al (1995), C. Baban, et al (2003), M. Nowak(1995). J.I. Pankove (1971)] have suggested different values of *m* for different glasses, $m = 2$ for most amorphous semiconductors (indirect transition) and $m = 1/2$ for most of crystalline semiconductor (direct transition). In the case of different thickness of polycrystalline of ZnTe thin films the direct and are valid. For higher values ($\alpha \geq 10^4$ cm^{-1}) the absorption coefficient, α (where the absorption is associated with interband transitions), the energy gap can be determined. Fig. 10 is a typical best fit of and $(\alpha(h\nu))^2$vs. photon energy (hν) for different thickness of ZnTe thin films. The values of the direct optical band gap E_g^{opt} were taken as the intercept of $(\alpha(h\nu))^2$ vs. $(h\nu)$ at $(\alpha(h\nu))^2 = 0$ for the allowed direct transition. The direct optical band gap derived increases from 2,16 to 2.22 eV wuth increasing the film thickness. The increase of $E_g^{opt}$for direct transition may be attributing to the increase in crystallites size. The increase of grain size with thickness can be attributed to the improved crystallinity. The improvement in crystallinity is due to increase ability of add atoms to move towards stable sites in the lattice.

© The authors. Published by Info Media Group & Anglisticum Journal, Tetovo, Macedonia.
Selection and peer-review under responsibility of ICNHBAS, 2013 http://www.nhbas2013.com

Thicker films are characterized by more homogeneous network, which minimizes the number of defects and localized states, and thus the optical band gap increases [E.A. Davis et al (1970), E.A. Fagen et al (1970), E.R. Shaaban et al (2007), S. K.Biswas et al (1986) , K.I. Arshak et al (1986)].

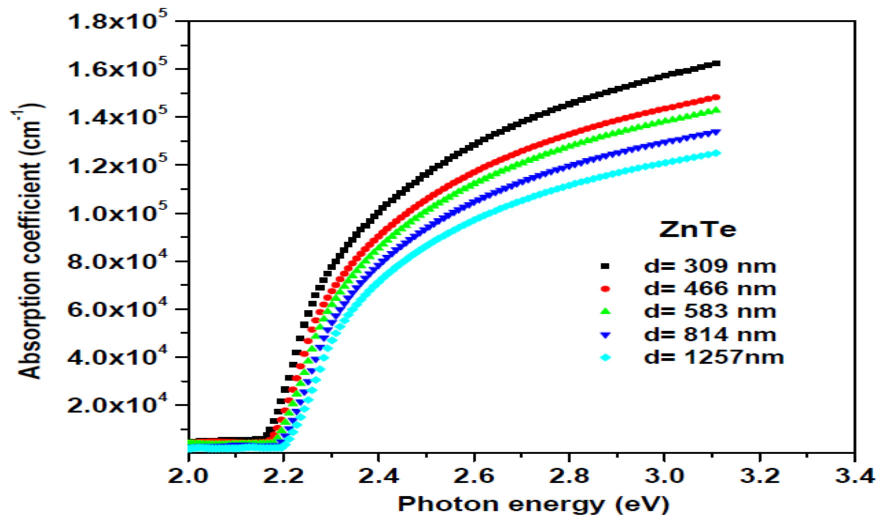

Fig.8. Variation of absorption coefficient α vs. $h\upsilon$ for ZnTe films with different thickness

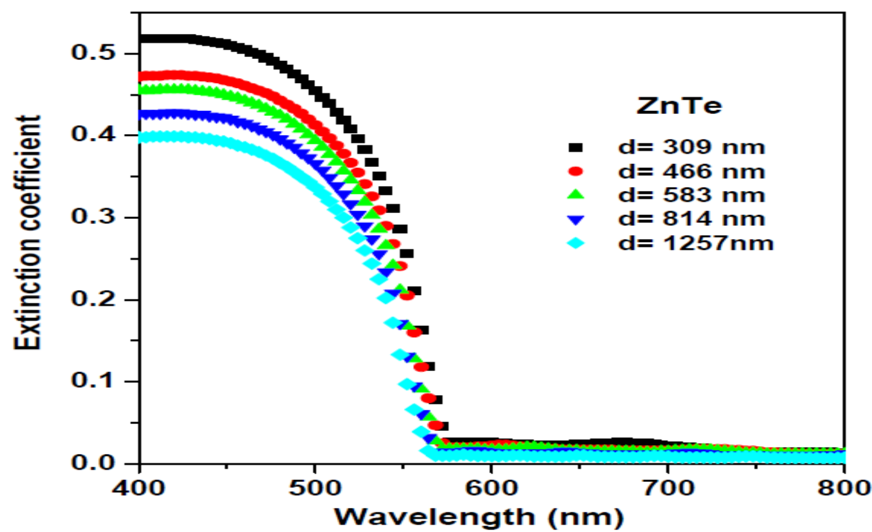

Fig.9. The spectral dependence of extinction coefficient *k* of ZnTe films with different thicknesses (*d*).

© The authors. Published by Info Media Group & Anglisticum Journal, Tetovo, Macedonia.
Selection and peer-review under responsibility of ICNHBAS, 2013 http://www.nhbas2013.com

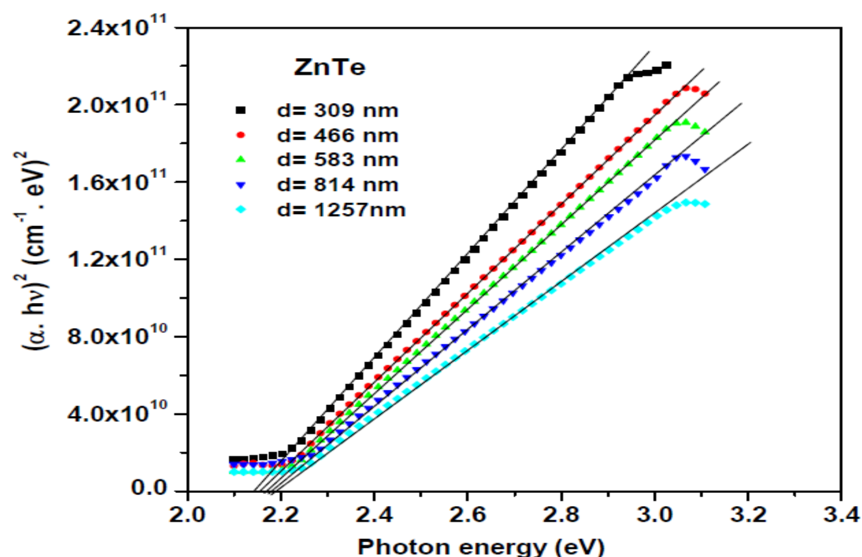

Fig.10. Variation of $(\alpha(h\nu))^2$ vs. $h\nu$ for ZnTe films with different thicknesses (d).

Table.1. Comparative look of the breadth, crystallite size and microstrain of ZnTe nanoparticle thin films with different thicknesses.

Thickness (nm)	$\beta(2\theta_0)$			Crystallite size D_v (nm)	Micro-Strain e X 10^{-3}
	(111)	(220)	(311)		
Powder	**0.2561**	**0.2691**	**0.2681**	-----	-----
309	0.546	0.629	0.6705	23.65	1.93
466	0.5258	0.6138	0.6453	24.99	1.916
583	0.491	0.5599	0.6055	27.95	1.812
814	0.456	0.524	0.5555	30.83	1.628
1257	0.4458	0.5188	0.5403	31.78	1.593

© The authors. Published by Info Media Group & Anglisticum Journal, Tetovo, Macedonia.
Selection and peer-review under responsibility of ICNHBAS, 2013 http://www.nhbas2013.com

Table. 2: Values of λ, T_M and T_m for different thickness of *ZnTe* thin films corresponding to transmission spectra of Figure 5; the values of transmittance are calculated by orgin program. The calculated values of refractive index and film thickness are based on the envelope method.

Samples	*λ*	T_M	*Tm*	*S*	n_1	$d_1(nm)$	m_0	*m*	$d_2(nm)$	n_2
	674	0.71	0.488	1.533	2.632	—	2.55	2.5	320.1	2.723
	798	0.765	0.521	1.538	2.601	343.9	2.128	2	306.8	2.579
	1010	0.802	0.569	1.54	2.475	309.1	1.6	1.5	306	2.448
	1426	0.832	0.617	1.531	2.341	—	1.072	1	304.6	2.305

$\bar{d}_2 = 309.4$ nm $\sigma_2 = 7.2$ nm (2.3 %)

Samples	*λ*	T_M	T_m	*S*	n_1	$d_1(nm)$	m_0	*m*	$d_2(nm)$	*n2*
	726	0.712	0.485	1.535	2.655	—	3.584	3.5	478.6	2.724
	816	0.741	0.507	1.538	2.617	516.5	3.143	3	467.7	2.624
	946	0.771	0.538	1.54	2.544	480.9	2.635	2.5	464.9	2.535
	1140	0.801	0.569	1.539	2.471	472.7	2.124	2	461.4	2.444
	1474	0.826	0.597	1.53	2.404	—	1.599	1.5	459.8	2.37

$\bar{d}_1 = 490.04$ nm $\sigma_1 = 23.28$ nm (4.7 %) $\bar{d}_2 = 466.48$ nm $\sigma_2 = 7.4$ nm (1.5%)

Samples	**λ**	T_M	Tm	***S***	n_1	$d_1(nm)$	m_0	***m***	$d_2(nm)$	n_2
	666	0.676	0.443	1.533	2.796	—	5.076	5	595.4	2.855
	718	0.692	0.462	1.535	2.731	644.2	4.598	4.5	591.6	2.77
	784	0.716	0.482	1.537	2.683	633.8	4.138	4	584.4	2.689
	870	0.741	0.506	1.539	2.623	599.5	3.644	3.5	580.5	2.611
	986	0.761	0.531	1.54	2.552	585.5	3.129	3	579.5	2.536
	1154	0.782	0.554	1.538	2.493	587.1	2.612	2.5	578.6	2.473
	1404	0.804	0.577	1.532	2.438	576.8	2.1	2	575.8	2.407
	1828	0.824	0.604	1.521	2.365	—	1.564	1.5	579.8	2.351

$\bar{d}_1 = 604.48$ nm $\sigma_1 = 27.89$ nm (4.7 %) $\bar{d}_2 = 583$ nm $\sigma_2 = 6.85$ nm (1.1 %)

Samples	***λ***	T_M	*Tm*	***S***	n_1	$d_1(nm)$	m_0	***m***	$d_2(nm)$	n_2
	712	0.677	0.446	1.535	2.784	—	6.587	6.5	831.3	2.844
	754	0.693	0.46	1.536	2.748	899.8	6.141	6	823.1	2.78
	806	0.71	0.476	1.538	2.703	854.2	5.651	5.5	819.9	2.724
	868	0.726	0.493	1.539	2.656	850.9	5.155	5	817.1	2.667
	944	0.742	0.509	1.54	2.611	839.3	4.661	4.5	813.4	2.611
	1042	0.758	0.526	1.54	2.567	833.1	4.151	4	811.8	2.561
	1166	0.773	0.542	1.538	2.526	831.7	3.649	3.5	807.9	2.508
	1334	0.788	0.559	1.534	2.485	818.8	3.138	3	805.3	2.459
	1570	0.802	0.574	1.527	2.442	811.2	2.621	2.5	803.6	2.412
	1930	0.813	0.587	1.52	2.405	—	2.1	2	802.4	2.372

$\bar{d}_1 = 842.37$ nm $\sigma_1 = 27.37$ nm (3.2 %) $\bar{d}_2 = 813.58$ nm $\sigma_2 = 9.34$ nm (1.14 %)

© The authors. Published by Info Media Group & Anglisticum Journal, Tetovo, Macedonia.
Selection and peer-review under responsibility of ICNHBAS, 2013 http://www.nhbas2013.com

Samples	λ	T_M	Tm	S	n_1	$d_1(nm)$	m_0	m	$d_2(nm)$	n_2
	746	0.677	0.451	1.536	2.755	—	9.567	9.5	1286	2.818
	776	0.688	0.46	1.537	2.733	1383	9.123	9	1278	2.777
	812	0.7	0.471	1.538	2.705	1353	8.63	8.5	1276	2.745
	850	0.711	0.481	1.539	2.679	1277	8.166	8	1269	2.704
	892	0.722	0.49	1.54	2.658	1346	7.718	7.5	1259	2.66
	946	0.733	0.501	1.54	2.631	1304	7.203	7	1259	2.633
	1002	0.742	0.511	1.54	2.601	1289	6.724	6.5	1252	2.59
	1074	0.754	0.523	1.539	2.57	1281	6.198	6	1254	2.563
	1154	0.764	0.534	1.538	2.545	1285	5.713	5.5	1247	2.524
	1256	0.773	0.544	1.536	2.517	1239	5.19	5	1248	2.497
	1380	0.781	0.554	1.533	2.487	1257	4.668	4.5	1249	2.469
	1532	0.79	0.564	1.528	2.46	1263	4.16	4	1245	2.437
	1732	0.799	0.573	1.523	2.435	1266	3.642	3.5	1245	2.411
	1998	0.808	0.581	1.52	2.42	—	3.137	3	1239	2.384

$\bar{d}_1$ = **1295.25 nm** σ_1 **=43.57 nm (3.36 %)** $\bar{d}_2$ = **1257.57 nm** σ_2 **= 14.36 nm (1.14 %)**

Conclusions

Different thickness of polycrystalline ZnTe films have been deposited onto glass substrates at room temperature by vacuum evaporation technique. From XRD studies it was found that the film is polycrystalline in nature with the ZnTe crystallites having the zinc blende structure. The calculated microstructure parameters of the ZnTe thin films such as crystallite size (Dv) and microstrain e showed that the size of crystallites increases with increasing the film thickness, while the microstrain shows an opposite variation trend due to the decrease in lattice defects, which were pronounced at small thicknesses. The envelope method suggested by Swanepoel has been applied to the films with a reasonable number of interference fringes. The optical method applied here makes it possible to determine the refractive index and average thickness of the films. The results indicate that the values of n gradually increase with increasing the film thickness up to 814 nm and then the variation of n with for higher thicknesses lies within theexperimental error. The increase of n with film thickness may be attributed the increase of crystallite size and decrease in microstrain which were found to more appreciable in the small range of film thickness. The direct optical band gap derived increases from 2.16 to 2.22 eV wuth increasing the film thickness. The increase of E_g^{opt} for direct transition may be attributing to the increase in crystallites size. The increase of grain size with thickness can be attributed to the improved crystallinity.

References

1. W.L.Wolfe, The infrared handbook, in:W.L.Wolfe, G.J. Zissis (Eds.), The Infrared Information and Analysis Center, Environmental Research Institute of Michigan, 1978.
2. J. De Merchant, M. Cocievera, J. Electrochem. Soc. 143 (1996) 4054.
3. Kaneta, S. Adachi, J. Phys., D, Appl. Phys. 33 (2000) 901.

© The authors. Published by Info Media Group & Anglisticum Journal, Tetovo, Macedonia.
Selection and peer-review under responsibility of ICNHBAS, 2013 http://www.nhbas2013.com

4. Pistone, A.S. Arico, P.L. Antonucci, D. Silvestro, V. Antonucci, Sol. Energy Mater. Sol. Cells 53 (1998) 255.
5. A.K.S. Aquili, Z. Ali, A. Maqsood, Appl. Surf. Sci. 167 (2000) 1.
6. Mondal, S. Chaudhuri, A.K. Pal, Appl. Phys., A 43 (1987) 81.
7. H. Bellakhder, A. Outzourhit, E.L. Ameziane, Thin Solid Films 265 (2001) 30.
8. R.L. Gunshor, L.A. Koladziejski, N. Otsuka, S. Dutta, Surf. Sci. 174 (1986) 522.
9. T. Ishizaki, T. Ohtomo, A. Fuwa, J. Phys., D, Appl. Phys. 37 (2004) 255.
10. C.T. Lynch (Ed.), Handbook of Materials Science, vol. 3, Chemical Rubber Company, Cleveland, OH, 1974, pp. 134– 142.
11. Coating Materials, Liechtenstein, Balzers, 1981, p. c7, edition.
12. A.A. Ibrahim, N.Z. El-Sayed, M.A. Kaid, A. Ashour, Vacuum 75 (2004) 189.
13. H. P. Klug, L. Alexander, X-ray diffraction procedures for polycrystalline and amorphous materials. 2nd ed. New York: John Wiley & Sons, 1974, [chapter 9]. p. 618-708.
14. G. K. Williamson, W. H., Hall Acta Metallurgica (1953);1:22-31.
15. D.G. Morris, M. A. Morris, M. LeBoeuf, Materials Science and Engineering A156(1992)11.
16. G. H. Chen, C. Suryanarayana, F. H. Froes, Metallurgical and Materials Transactions 26A (1995) 1379.
17. F. W. Gayle, F. S. Biancaniello, NanoStructured Materials 6 (1995)429.
18. E. Szewczak, J. Paszula, A. V. Leonov, H. Matyja, Materials Science and Engineering A226-228 (1997) 115.
19. R. Swanepoel R, J. Phys. E: Sci. Instrum., 17 896 (1984).
20. A.K. Kulkarnia, K.H. Schulzb, T. S. Lima, M. Khanb, Thin Solid Films 308–309 (1997) 1
21. E. R. Shaaban, M.El-Hagary, M. Emam-Ismailad, M. B. El-Den, Phil.Mag. 91 (12) (2011) 1692.
22. E. Márquez, J.M. González-Leal, A.M. Bernal-Oliva, R. Jiménez-Garay and T. Wagner, Journal of Non-Crystalline Solids, 354 (2008) 503.
23. E.R. Shaaban, M.A. Kaid, E.S. Moustafa, A. Adel, J. Phys. D: Appl. Phys. 41 (2008) 125301.
24. E. R. Shaaban, Philosophical Magazine, 88 781 (2008).
25. M. Kastner, *Phys. Rev Lett*. 28 (1972) 355.
26. L.L. Kazmersky (Ed.), Polycrystalline and Amorphous Thin Films and Devices, Academic Press, New York, 1980, pp. 135–152.
27. R. Swanepoel, J. Phys. E: Sci. Instrum. 16 (1983) 121; 17 (1984) 896.
28. E. Marques, J.B. Ramerez-Malo, P. Villares, R. Jimenez-Garay, R. Swanepoel, Thin Solid Films 254 (1995) 83.
    A. Baban, G.I. Rusu, Appl. Surf. Sci. 211 (2003) 6.
29. M. Nowak, Thin Solid Films 266 (1995) 258.
30. J.I. Pankove, Optical Processes in Semiconductors, Dover, New York, (1971) 44.
31. E.A. Davis, N.F. Mott, Philos. Mag. 22 (1970) 903.
32. E.A. Fagen, H. Fritzsche, J. Non-Cryst. Solids 2 (1970)180.
33. E.R. Shaaban, M. Abdel-Rahman, El Sayed Yousef, M.T. Dessouky. Thin Solid Films 515 (2007) 3810.
34. S. K.Biswas, S. Chaudhuri, A. Choudhury, Phys. Status. Solidi (a), 105 (1988) 467.
35. K.I. Arshak, C. Ahogarth, Thin Solid Films 137 (1986) 281.

© The authors. Published by Info Media Group & Anglisticum Journal, Tetovo, Macedonia.
Selection and peer-review under responsibility of ICNHBAS, 2013 http://www.nhbas2013.com